Finite-width Laplacian sum rules for 2^{++} tensor glueball in the instanton vacuum model

Junlong Chen and Jueping Liu*

College of Physics and Technology, Wuhan University, Wuhan 430072, China

(Received 19 October 2016; published 23 January 2017)

The more carefully defined and more appropriate 2^{++} tensor glueball current is a $SU_c(3)$ gauge-invariant, symmetric, traceless, and conserved Lorentz-irreducible tensor. After Lorentz decomposition, the invariant amplitude of the correlation function is abstracted and calculated based on the semiclassical expansion for quantum chromodynamics (QCD) in the instanton liquid background. In addition to taking the perturbative contribution into account, we calculate the contribution arising from the interaction (or the interference) between instantons and the quantum gluon fields, which is infrared free. Instead of the usual zero-width approximation for the resonances, the Breit-Wigner form with a correct threshold behavior for the spectral function of the finite-width three resonances is adopted. The properties of the 2^{++} tensor glueball are investigated via a family of the QCD Laplacian sum rules for the invariant amplitude. The values of the mass, decay width, and coupling constants for the 2^{++} resonance in which the glueball fraction is dominant are obtained.

DOI: 10.1103/PhysRevD.95.014024

I. INTRODUCTION

Within the framework of quantum chromodynamics (QCD), the hadron spectrum is expected to be more complex than the prediction of the usual quark model. The gluons (which mediate the strong interactions) carry color charges and interact among themselves, so that a particular type of bound state—glueballs—should exist even in the quarkless world. The study of glueballs may give a unique insight into the non-Abelian dynamics of QCD. Theoretical investigations—including lattice simulations [1–3], model researches [4–6], and sum-rule analyses [7–18]—have been going on for a long time, but no decisive evidence of the existence of glueballs has been confirmed by experimental research up to now [19,20]. Further investigation on glueballs still makes sense.

One of the obstacles in the theoretical study of glueballs is that the nonperturbative dynamics of QCD—which is responsible for the formation of hadrons—is difficult to handle. In particular, the tunneling effect between the degenerate vacua of QCD should be taken into account. In the leading order, this effect is described by instantons [21,22] and shown to be of great significance in generating the properties of the unusual hadrons (glueballs). Now, the QCD vacuum is recognized to be a medium with nontrivial structure, and it may have a large impact on the attributes of hadrons. Moreover, the glueball may be mixed with usual mesons of the same quantum numbers, making the identification of the glueballs more complicated [12,23].

Instantons, as the strong topological fluctuations of gluon fields in QCD, are widely believed to play an important role in the physics of the strong interaction (for reviews, see Refs. [22,24]). In particular, instantons provide mechanisms for the violation of both $U(1)_A$ and chiral symmetry in QCD, and may therefore be important in determining hadron masses and the resolution of the famous $U(1)_A$ problem. Furthermore, it was recently shown that instantons persist through the deconfinement transition, so that instanton-induced interactions between quarks and gluons may underlie the unusual properties of the so-called strongly coupled quark-gluon plasma recently discovered at RHIC [25].

In conventional perturbation theory one computes fluctuations around the trivial zero solution. The correct quantization process is to consider all classical solutions of the field equations and their quantum fluctuations. In the path integral representation of QCD the partition function is, hence, dominated by an ensemble of extended particles (instantons) in four dimensions. In the simplest case the partition function describes a diluted ideal gas of independent instantons. Unfortunately, this assumption leads to an infinite instanton density caused by large instantons, which is obviously against the dilution gas hypothesis for instantons. This problem is called the infrared problem.

The problem is avoided by assuming a repulsive interaction between instantons [26] which prevents the collapse. This is the model of a four-dimensional instanton liquid. Under certain circumstances the interaction can be replaced by an effective density. The instanton liquid model in a narrow sense describes the QCD vacuum as a sum of independent instantons with radius $\overline{\rho} = (600\ \mathrm{MeV})^{-1}$ and effective density $\overline{n} = (200\ \mathrm{MeV})^4$. The correctness of this model is still being intensively investigated. So far the model is essentially justified by its phenomenological successes. The most important predictions of the model

*To whom all correspondence should be addressed.
jpliu@whu.edu.cn

are probably the breaking of the chiral symmetry in the axial triplet channel [27,28] and the absence of Goldstone bosons in the axial singlet channel.

The instanton distribution is closely connected with the vacuum condensates, which have been proposed as the nonperturbative effects of QCD arising from the nontrivial vacuum, since the mean size and density of instantons can be deduced from the quark and gluon condensates and vice versa. Moreover, the values of condensates can be reproduced from the instanton distribution [29–32]. The contributions of instantons and those of the condensates may reveal the same nonperturbative effects, and thus including both contributions at the same time will cause the so-called double-counting problem [33]. To avoid it, a semiclassical expansion in instanton background fields was suggested in our previous works to analyze the properties of the lowest 0^{++} scalar glueball [13,34] and 0^{-+} pseudoscalar one [15–18], where the correlation functions of the glueball currents are calculated by just including the contributions from the pure instantons, the pure quantum gluons, and the interference between both, instead of working with both instantons and condensates at the same time. In fact, the condensate contributions turned out to be very small as compared with those of instantons (including the classical and quantum interference contributions) in the glueball channels, and may be understood as a small fraction of the latter in the local limit [13,15,16].

In this paper, we investigate the mass scale and the magnitude of the width for the lowest state of tensor glueballs along the same line with our previous works [13–18]. This issue was first considered in a nonrelativistic approach by assuming a large value of the effective gluon mass [35], and the mass $m_{2^{++}}$ of the lowest tensor glueball was predicted to be about 1.6 GeV; later, relying on the construction of an efficient quasiparticle gluon basis for Hamiltonian QCD in Coulomb gauge, $m_{2^{++}}$ was determined to be 2.42 GeV. The lattice simulation on an anisotropic lattice for quenched QCD shows that the mass of the lowest state of the tensor glueballs is about 2.3–2.4 GeV [36,37]. The first prediction of the traditional QCD sum-rule approach was $m^2_{2^{++}} \approx 1.6\ \mathrm{GeV}^2$ [38,39]. By assuming very small mixing between the tensor glueball and quarkonia, the sum-rule prediction was increased to $m_{2^{++}} \approx 2.00$ GeV [40,41]. Up to now, the theoretical results have been controversial. Finally, let us mention that the prediction in the flux tube model—being composed of a closed loop of fundamental flux with no constituent gluons at all—is $m_{2^{++}} \approx 2.84$ GeV [42].

Our paper is organized as follows. In Sec. II we define our form for the current of the tensor glueball and the corresponding correlation function, and make its Lorentz decomposition and associate it with a unique Lorentz-invariant amplitude. In Sec. III a low-energy theorem suitable for the correlation function is derived. The pure quantum and pure instanton contributions (including the traditional condensate one) are presented in Sec. IV. Our main work—namely, the calculation of the interference contribution—is carried out in Sec. V. In Sec. VI we construct the spectral function for the invariant amplitude of the correlation function. The finite-width Laplacian sum rules—which we also used in our previous works—are presented in Sec. VII. The numerical simulation is described in Sec. VIII. Finally, in Sec. IX our results and conclusions are summarized, and a discussion of some issues is given.

II. THE CORRELATION FUNCTION AND ITS LORENTZ DECOMPOSITION

The current composed of two gluon fields, which carries the quantum numbers $J^{PC} = 2^{++}$, is defined as

$$O_{\mu\nu} = \eta_{\mu\alpha}(\partial)\eta_{\nu\beta}(\partial)\alpha_s\theta_{\alpha\beta}, \tag{1}$$

with

$$\theta_{\alpha\beta} = \left[-G^a_{\alpha\gamma}G^a_{\beta\gamma} + \frac{1}{4}\delta_{\alpha\beta}G^a_{\gamma\delta}G^a_{\gamma\delta}\right]_- \tag{2}$$

being the traceless energy-momentum density tensor in Euclidean pure QCD, where $G^a_{\mu\nu}$ is the gluon field strength tensor with the color index a and Lorentz indices μ and ν, and $\eta_{\mu\nu}(\partial) = \delta_{\mu\nu} - \partial_\mu\partial_\nu/\partial^2$ is the transverse projection operator. It is important to note that the overall subscript "$-$" on the rhs of Eq. (2) indicates that the corresponding trace anomaly should be deleted, and this subscript will not be specified hereafter. The current $O_{\mu\nu}$ is a Lorentz-irreducible, $SU_c(3)$ gauge-invariant, and local composite operator with the lowest dimension. Obviously, $O_{\mu\nu}$ is also a Lorentz-symmetric traceless tensor obeying the transverse condition

$$O_{\mu\nu} = O_{\nu\mu}, \qquad O_{\mu\mu} = 0, \qquad \partial_\mu O_{\mu\nu} = 0, \tag{3}$$

where the third equation is valid not only in pure QCD but also in full QCD by means of using the projection operator $\eta_{\mu\nu}(\partial)$.

The QCD correlation function of the current $O_{\mu\nu}$ is defined as

$$\Pi_{\mu\nu,\mu'\nu'}(q) = \int d^4x e^{iq\cdot x}\langle\Omega|TO_{\mu\nu}(x)O_{\mu'\nu'}(0)|\Omega\rangle. \tag{4}$$

Equation (3) leads to the symmetric, traceless, and transverse conditions for $\Pi_{\mu\nu,\mu'\nu'}(q)$ as follows:

$$\begin{aligned}
&\Pi_{\mu\nu,\mu'\nu'}(q) = \Pi_{\nu\mu,\mu'\nu'}(q) = \Pi_{\mu\nu,\nu'\mu'}(q),\\
&\Pi_{\mu\mu,\mu'\nu'}(q) = \Pi_{\nu\mu,\mu'\mu'}(q) = 0,\\
&\partial_\mu\Pi_{\mu\nu,\mu'\nu'}(q) = \partial_{\mu'}\Pi_{\mu\nu,\mu'\nu'}(q) = 0.
\end{aligned} \tag{5}$$

For any momentum q, there is a unique transverse symmetric Lorentz tensor in Euclidean space-time, namely,

$$\eta_{\mu\nu}(q) = \delta_{\mu\nu} - \frac{q_\mu q_\nu}{q^2}. \tag{6}$$

By means of $\eta_{\mu\nu}(q)$, it is easy to find that there are only two possible Lorentz tensors of rank four that satisfy the symmetric and transverse conditions shown in Eq. (5):

$$\begin{aligned} T^{(1)}_{\mu\nu,\mu'\nu'} &= \eta_{\mu\nu}(q)\eta_{\mu'\nu'}(q), \\ T^{(2)}_{\mu\nu,\mu'\nu'} &= \eta_{\mu\mu'}(q)\eta_{\nu\nu'}(q) + \eta_{\mu\nu'}(q)\eta_{\nu\mu'}(q). \end{aligned} \tag{7}$$

Then, the traceless Lorentz tensor of rank four, $\eta_{\mu\nu,\mu'\nu'}$, can be expressed as the linear combination of the above two tensors:

$$\eta_{\mu\nu,\mu'\nu'} = \eta_{\mu\mu'}\eta_{\nu\nu'} + \eta_{\mu\nu'}\eta_{\nu\mu'} - \frac{2}{3}\eta_{\mu\nu}\eta_{\mu'\nu'}, \tag{8}$$

where the factor $-2/3$ in front of the third term is determined by the traceless condition, and the argument q of η is ignored from now on for the sake of brevity. It is important to note that $\eta_{\mu\nu,\mu'\nu'}$ is the unique Lorentz tensor of the fourth rank constructed from q and $\delta_{\mu\nu}$, and it is proportional to the density matrix of spin two possessing the desired properties of Eq. (5). We conclude that the correlation function $\Pi_{\mu\nu,\mu'\nu'}(q)$ can be expressed as

$$\Pi_{\mu\nu,\mu'\nu'}(q) = \frac{1}{10}\eta_{\nu\mu,\mu'\nu'}\Pi(q^2), \tag{9}$$

with $\Pi(q^2)$ being a scalar function of q^2, and we introduce the factor of $\frac{1}{10}$ for convenience. By contracting both sides of Eq. (9) with the product of the metric tensors $\delta_{\mu\mu'}\delta_{\nu\nu'}$ and using the identity $\delta_{\mu\mu'}\delta_{\nu\nu'}\eta_{\nu\mu,\mu'\nu'} = 10$, we have

$$\Pi(q^2) = \Pi_{\mu\nu,\mu\nu}(q), \tag{10}$$

which is the Lorentz-invariant amplitude that our sum rule is, of course, written for.

III. LOW-ENERGY THEOREM

To compare with the scalar and pseudoscalar cases of glueballs, we want to evaluate the correlation function in the low-energy limit of q,

$$\lim_{\text{low } q}\Pi(q^2) = \lim_{\text{low } q}\int d^4x e^{iq\cdot x}\langle\Omega|TO_{\mu\nu}(x)O_{\mu\nu}(0)|\Omega\rangle. \tag{11}$$

We note that the current O is the energy-momentum tensor in pure QCD which is symmetric and conserved according to our definition, and so it is in fact renormalization group invariant at least at one-loop order.

Now, it is noticed that the renormalization group invariance of O enables us to extrapolate it to a low-energy scale, at which it may be reduced to the symmetric and conserved energy-momentum tensor in the low-energy limit of QCD. On the other hand, the $1/N_c$ expansion indicates that the confinement is present for large N_c, and in the region of confinement the fundamental theory of QCD is reduced to a weakly coupled field theory of mesons, such as pions [43,44]. Therefore, at the low-energy scale, the energy-momentum tensor of QCD may be reduced to the symmetric and conserved energy-momentum tensor for the pion field theory at the leading order,

$$O^{(\pi)}_{\mu\nu} = \partial_\mu\pi^a\partial_\nu\pi^a - \frac{1}{2}\delta_{\mu\nu}[\partial_\alpha\pi^a\partial_\alpha\pi^a - m_\pi^2\pi^2], \tag{12}$$

where π^a is the pion isotopic amplitude ($\pi^a\pi^a = \pi^0\pi^0 + 2\pi^+\pi^-$). In fact, the low-energy energy-momentum tensor (12) is Lorentz reducible, and its nonvanishing trace (possessing no projection on the 2^{++} state) should be deleted according to our definition. The traceless part of $O^{(\pi)}_{\mu\nu}$ is

$$O^{(\pi)}_{\mu\nu-} = \partial_\mu\pi^a\partial_\nu\pi^a - \frac{1}{4}\delta_{\mu\nu}\partial_\alpha\pi^a\partial_\alpha\pi^a. \tag{13}$$

Inserting the two-pion intermediate states between the two currents on the rhs of Eq. (11), using Eq. (13), we obtain

$$\lim_{\text{low } q}\Pi(q^2) = 10\times 2\times\frac{3}{4}m_\pi^4\theta(q^2 - 4m_\pi^2), \tag{14}$$

where the factor 10 is introduced by convention [see Eqs. (9) and (10)], and the factor of 2 comes from the multiplicity of the pion isotopic states π^a with the approximate equal mass m_π. We note that the appearance of a step function $\theta(q^2 - 4m_\pi^2)$ is due to the consideration of the energy conservation. For the finiteness of the pion mass, we have

$$\lim_{q\to 0}\Pi(q^2) = \int d^4x\langle\Omega|TO^{(\pi)}_{\mu\nu-}(x)O^{(\pi)}_{\mu\nu-}(0)|\Omega\rangle = 0, \tag{15}$$

without consideration of the possibility of a 2^{++} meson or glueball decaying into two photons.

There is also another argument for the low-energy theorem (15) for the tensor glueball current. Inserting the full intermediate states into the correlation function between the two currents $O_{\mu\nu}(x)$ and $O_{\mu\nu}(0)$, it is easy to see that all intermediate states have no contribution, with the possible exceptions of the vacuum $|\Omega\rangle$ and the multimassless pions $|n\pi\rangle$ with $n = 2, 4, \cdots$ due to energy-momentum conservation. The intermediate vacuum state has no contribution,

$$\langle\Omega|O^{(\pi)}_{\mu\nu-}(0)|\Omega\rangle = \frac{1}{4}\delta_{\mu\nu}\langle\Omega|O^{(\pi)}_{\alpha\alpha-}(0)|\Omega\rangle = 0, \quad (16)$$

where the first equality is due to the Lorentz covariance, and the second equality comes from our definition of our current O which is exactly traceless. The intermediate multipion states $|n\pi\rangle$ do not contribute as well, since n pions—each of which has vanishing energy and momentum in the massless limit—cannot possess the total angular momentum of two so that

$$\langle n\pi|O^{(\pi)}_{\mu\nu-}(0)|\Omega\rangle_{m_\pi=0,q\to 0} = 0,$$

in keeping the angular momentum conservation.

IV. PURE QUANTUM AND PURE INSTANTON CONTRIBUTIONS

We work in the framework of the semiclassical expansion to evaluate the Euclidian path integrals, as in lattice QCD. Instead of using the global minimum of the QCD action ($A_\mu = 0$) as the starting point in the usual perturbation theory, we may use the local minima (instantons) $A_\mu(x)$, which are the nonperturbative solutions of the classical field equations of Euclidean QCD with a finite action, so that the glue potential field $B(x)$ may be decomposed into a summation of the classical instanton A and the corresponding quantum gluon field a as

$$B_\mu(x) = A_\mu(x) + a_\mu(x). \quad (17)$$

Consequently, the pure-glue Euclidean action can be expressed as

$$\begin{aligned} S[B] &= S_0 - \int \mathrm{d}^4x\left\{L[A+a] + \frac{1}{2\xi}a_{a\mu}D_{ab\mu}D_{bc\nu}a_{c\nu}\right\} \\ &= S_0 - \frac{1}{2}\int \mathrm{d}^4x\left\{a_{a\mu}\left[D_{ab\lambda}D_{bc\lambda}\delta_{\mu\nu} + 2gf_{abc}F_{b\mu\nu}\right.\right. \\ &\quad \left.\left. - \left(1-\frac{1}{\xi}\right)D_{ab\mu}D_{bc\nu}\right]a_{c\nu} - 2gf_{abc}a_{b\mu}a_{c\nu}D_{ad\mu}a_{d\nu} \right. \\ &\quad \left. - \frac{1}{2}g^2 f_{abc}a_{b\mu}a_{c\nu}f_{ade}a_{d\mu}a_{e\nu}\right\}, \end{aligned} \quad (18)$$

where $S_0 = 8\pi^2/g^2$ is the one-instanton contribution to the action, $F_{a\mu\nu}$ is the instanton field-strength tensor

$$F_{a\mu\nu}(A) = \partial_\mu A_{a\nu} - \partial_\nu A_{a\mu} + g_s f_{abc}A_{b\mu}A_{c\nu}, \quad (19)$$

and $D_{ab\mu}(A)$ is the covariant derivative associated with the classical instanton field $A_{a\mu}$,

$$D_{ab\mu}(A) = \partial_\mu\delta_{ab} + gf_{acb}A_{c\mu}. \quad (20)$$

In addition, following 't Hooft [21], the background field gauge

$$D_\mu(A)a_\mu = 0 \quad (21)$$

is used, with ξ being the corresponding gauge parameter, and certainly the corresponding Faddeev-Popov ghosts according to the standard rule should be added to restore unitarity. We note here that the structure constants f_{abc} should be understood as ϵ_{abc} when any one of the color indices (a, b, or c) is associated with an instanton field due to the property of the closure of any group.

According to the decomposition (17), the invariant amplitude of the correlation function splits into three parts, namely, the pure classical part, the pure quantum part, and the interference part in the leading order,

$$\Pi^{\mathrm{QCD}} = \Pi^{(\mathrm{cl})} + \Pi^{(\mathrm{qu})} + \Pi^{(\mathrm{int})}, \quad (22)$$

where the superscript indicates that it is calculated in the underlying dynamical theory (QCD). It is important to note that every part on the rhs of Eq. (22) is gauge-invariant because the decomposition (17), in principle, has no impact on the gauge invariance of the correlation function.

The first part of Eq. (22) arises from the contribution of pure classical field configurations—the Belavin-Polyakov-Schwarz-Tyupkin instanton and anti-instanton—which are the simplest nonperturbative solutions of the Euclidean pure-QCD field equation, and the instanton field is written (in the singular gauge) as

$$A_{a\mu}(x) = \frac{2}{g_s}\eta_{a\mu\nu}(x-z)_\nu\phi(x-z), \quad (23)$$

with

$$\phi(x-z) = \frac{\rho^2}{(x-z)^2[(x-z)^2+\rho^2]}, \quad (24)$$

and the corresponding field-strength tensor is

$$\begin{aligned} F_{a\mu\nu}(x) = -\frac{8}{g_s}&\left[\frac{(x-z)_\mu(x-z)_\rho}{(x-z)^2} - \frac{1}{4}\delta_{\mu\rho}\right] \\ &\times \eta_{a\nu\rho}\frac{\rho^2}{[(x-z)^2+\rho^2]^2} - (\mu\leftrightarrow\nu), \end{aligned} \quad (25)$$

where z and ρ denote the center and size of the instanton, respectively, which are called collective coordinates together with the color orientation, and $\eta_{a\mu\nu}$ is the 't Hooft symbol which should be replaced with the anti–'t Hooft one $\overline{\eta}_{a\mu\nu}$ for an anti-instanton field. The fact that the strong coupling constant g_s appears in the denominator of the rhs of Eq. (23) reveals the nonperturbative nature of these classical configurations. However, at the leading order, the so-called direct instantons do not contribute to the correlation function considered [7,38], namely,

$$\Pi^{(\mathrm{cl})} = 0, \quad (26)$$

because

$$\theta_{\alpha\beta}(F) = -F^a_{\alpha\gamma}F^a_{\beta\gamma} + \frac{1}{4}\delta_{\alpha\beta}F^a_{\gamma\delta}F^a_{\gamma\delta} = 0, \tag{27}$$

as expected for vacuum fields, for which the energy-momentum tensor should vanish.

The second part of Eq. (22) arises from the pure quantum contribution, and has already been calculated at the leading order [38],

$$\Pi^{(\mathrm{qu})} = -\frac{1}{2\pi^2}q^4 \ln\frac{q^2}{\mu^2}, \tag{28}$$

with μ being the renormalization scale, and with the additional ordinary power corrections due to the gluon condensates

$$\Pi^{(\mathrm{cond})} = \frac{50\pi\alpha_s}{3q^4}\langle 2O_1 - O_2\rangle, \tag{29}$$

where

$$O_1 = (f^{abc}G^b_{\mu\alpha}G^c_{\nu\alpha})^2, \qquad O_2 = (f^{abc}G^b_{\mu\nu}G^c_{\alpha\beta})^2, \tag{30}$$

with f^{abc} being the structure constants for $SU_c(3)$. We note that the contribution from the vacuum condensates starts with the Q^{-8} term, and in fact is negligible (as checked in Fig. 5 in Appendix C) in comparison with the Borel transformations of $\Pi^{(\mathrm{int})}$, $\Pi^{(\mathrm{qu})}$, and $\Pi^{(\mathrm{cond})}$.

V. THE INTERFERENCE CONTRIBUTION

One of our main tasks in this work is to calculate the contribution $\Pi^{(\mathrm{int})}$ in Eq. (22), which comes from the interference between the classical instantons and quantum gluons in the framework of the semiclassical expansion for QCD with the instanton background, and which is certainly very important because of the vanishing pure-classical contribution (26). After imposing the background covariant Feynman gauge ($\xi = 1$) for the quantum gluon fields, we are still free to choose a gauge for the background field A. In the following, the singular gauge is chosen for the nonperturbative instanton field configurations, as shown in Eq. (23).

Before starting with the contraction between the quantum fields, we note that the time development of the instanton vacuum produces the preexponential factor for the distribution of the instantons [21,45,46], and $\Pi^{(\mathrm{int})}$ is understood as taking the ensemble average over the collective coordinates in addition to taking the usual vacuum expectation value due to the separation (23),

$$\Pi^{(\mathrm{int})} = \sum_{I,\bar{I}}\int d\rho n(\rho)\int d^4z\int d^4x e^{iq\cdot x} \times \langle\Omega|T\{O_{\mu\nu}(x)O_{\mu\nu}(0)\}^{(\mathrm{int})}|\Omega\rangle, \tag{31}$$

where the superscript "(int)" indicates that the corresponding quantity only contains the interference part between the quantum and classical ones. Using the spike distribution for the random instantons, Eq. (31) becomes

$$\Pi^{(\mathrm{int})} = 2\bar{n}\int d^4z\int d^4x e^{iq\cdot x} \times \langle\Omega|T\{O_{\mu\nu}(x)O_{\mu\nu}(0)\}^{(\mathrm{int})}|\Omega\rangle, \tag{32}$$

where the value of the instanton effective density $\bar{n}$ is already given in the introduction, and the factor of 2 comes from the mutually equal contributions of both the instanton and anti-instanton. The next important step is to specify the form of the gluon propagator which in the background-field Feynman gauge can be read from the part of $S[B]$ quadratic in a [47,48],

$$\mathcal{D}^{ab}_{\mu\nu}(x,y) = \langle\Omega|T\{a^a_\mu(x)a^b_\nu(y)\}|\Omega\rangle = \langle x|\left(\frac{1}{P^2\delta_{\mu\nu} - 2F_{\mu\nu}}\right)^{ab}|y\rangle, \tag{33}$$

with $P^{ab}_\mu = -iD^{ab}_\mu$. Keeping only terms proportional to F, one has [49]

$$\int d^4x e^{iq\cdot x}\mathcal{D}^{ab}_{\mu\nu}(x,y) = e^{iq\cdot(y-z)}\delta_{ab}\left\{\frac{1}{q^2}\delta_{\mu\nu} + g_s\frac{2}{q^4}F_{\mu\nu}(z) - ig_s\frac{(y-z)_\rho F_{\rho\sigma}(z)q_\sigma}{q^4}\delta_{\mu\nu}(z) + \cdots\right\}, \tag{34}$$

where the first term on the rhs of the above equation is the pure-gluon propagator in the usual Feynman gauge, and the second and third terms are the leading contribution of the instanton field to the gluon propagator. For the short-distance region, we assume that the contribution from a single instanton is dominant over multi-instantons [50]. At the leading loop level, the gluon propagator (33) in the background-field Feynman gauge becomes the pure-gluon one in the usual Feynman gauge, which is what we use in our calculation.

Rewriting the tensor glueball current (1) as

$$O_{\mu\nu} = \tilde{O}_{\mu\nu} - \frac{1}{4}\delta_{\mu\nu}\tilde{O}_{\alpha\alpha}, \tag{35}$$

with

$$\tilde{O}_{\mu\nu} = -G_{a\mu\alpha}G_{a\nu\alpha}, \tag{36}$$

the invariant amplitude (32) becomes

$$\Pi^{(\mathrm{int})} = 2\bar{n}\left(\delta_{\mu\mu'}\delta_{\nu\nu'} - \frac{1}{4}\delta_{\mu\nu}\delta_{\mu'\nu'}\right)\int d^4z \times\int d^4x e^{iq\cdot x}\langle\Omega|T\{\tilde{O}_{\mu\nu}(x)\tilde{O}_{\mu'\nu'}(0)\}|\Omega\rangle. \tag{37}$$

In our calculation, we expand $\tilde{O}_{\mu\nu}$ into terms which are products of quantum gluon fields and their derivatives with coefficients being composed of the instanton fields,

$$\tilde{O}_{\mu\nu} = \sum_{i=1}^{10} \tilde{O}_{\mu\nu}^{(i)}, \tag{38}$$

where the operators $\tilde{O}_{\mu\nu}^{(i)}$ in terms of the instanton and quantum gluon fields are listed in Appendix A. Then, Eq. (37) can be expressed as

$$\begin{aligned}\Pi^{(\mathrm{int})} &= 2\overline{n}\left(\delta_{\mu\mu'}\delta_{\nu\nu'} - \frac{1}{4}\delta_{\mu\nu}\delta_{\mu'\nu'}\right) \\ &\quad \times \sum_{i,j}\int d^4z \int d^4x \\ &\quad \times e^{iq\cdot x}\langle\Omega|T\{\tilde{O}_{\mu\nu}^{(i)}(x)\tilde{O}_{\mu'\nu'}^{(j)}(0)\}|\Omega\rangle \\ &= \sum_{i=1}^{12}\Pi_i^{(\mathrm{int})} + \cdots,\end{aligned} \tag{39}$$

where $\cdots$ denotes the contributions from the products of operators that are proportional to g_s^3, and the expressions for $\Pi_i^{(\mathrm{int})}$ are shown in Appendix B. The corresponding 12 kinds of Feynman diagrams are shown in Fig. 1, where the contributions from the first three diagrams are of the order of α_s, the contributions of the remainders are superficially of the order of α_s^2, and those from diagrams 4 and 6 are in fact vanishing as they violate the conservation of color charge, namely,

$$\Pi_i^{(\mathrm{int})} = 0, \quad \text{for } i = 4, 6. \tag{40}$$

Now, we are in the position to evaluate the contributions of the remainder diagrams in Fig. 1. Using the standard technique to regularize the ultraviolet divergence in the modified minimal subtraction scheme, the result for the interference part of the correlation function is

$$\begin{aligned}\Pi^{(\mathrm{int})} = \overline{n}\Big\{ & c_1\pi\alpha_s^{-1}(\mu^2) + c_2\pi(q\rho)^{-2}\alpha_s^{-1}(\mu^2) + c_3 \\ & + c_4(q\rho)^{-2} + [c_5(q\rho)^2 + c_6 + c_7(q\rho)^{-2}]\ln\frac{q^2}{\mu^2}\Big\},\end{aligned} \tag{41}$$

where μ is the renormalization scale, we have ignored terms that are proportional to the positive powers of q^2 which vanish after Borel transformation, and (after a tedious calculation) the dimensionless coefficients c_i are

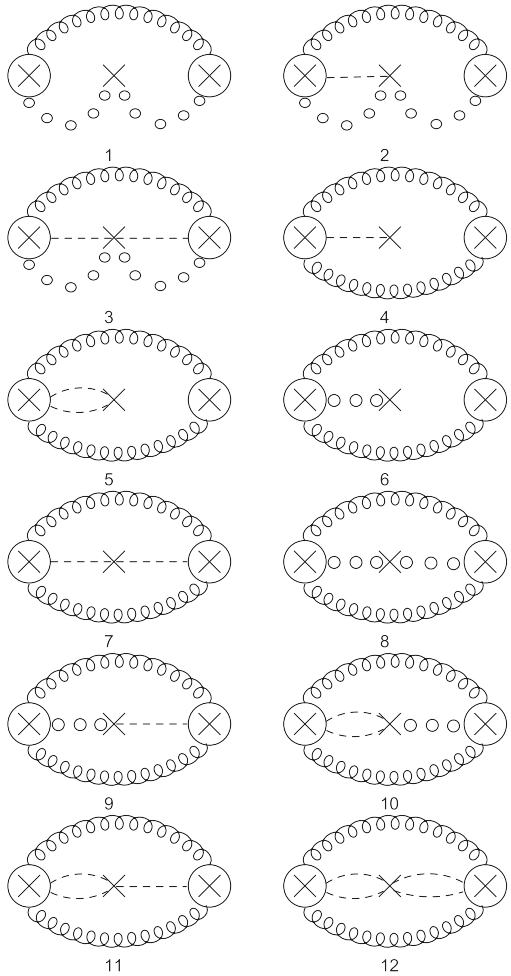

FIG. 1. Feynman diagrams for the interference contribution $\Pi^{(\mathrm{int})}$, where spiral lines, dotted lines, and the lines with circles denote gluons, instantons, and the instanton field-strength tensor, respectively, and crosses stand for the positions of the instantons.

$$\begin{aligned}c_1 &= 48, \\ c_2 &= -144, \\ c_3 &= -764 + \frac{664}{3}(\gamma - \ln 4\pi) = -1196.44, \\ c_4 &= -4416, \\ c_5 &= 27, \\ c_6 &= 364 - 140(\gamma - \ln 4\pi) = 637.53, \\ c_7 &= 2208,\end{aligned} \tag{42}$$

where γ is the Euler constant. The detailed calculation will appear elsewhere. It should be noted that there is no infrared divergence, as expected due to the instanton size being fixed in the liquid instanton vacuum model, which actually provides the regularization for the interference correlation function with the standard parameters.

Putting everything above together, our final expression for the invariant amplitude Π^{QCD} calculated in QCD is of the form

$$\Pi^{\rm QCD}(q^2) = \overline{n}\Big\{ c_1\pi\alpha_s^{-1}(\mu^2) + c_2\pi(q\rho)^{-2}\alpha_s^{-1}(\mu^2) + c_3 + c_4(q\rho)^{-2} + [c_5(q\rho)^2 + c_6 + c_7(q\rho)^{-2}]\ln\frac{q^2}{\mu^2}\Big\} - \frac{1}{2\pi^2}q^4\ln\frac{q^2}{\mu^2}, \quad (43)$$

where the condensate contribution $\Pi^{\rm cond}$ given in Eqs. (29) and (30) is neglected due to its small magnitude, as shown in Appendix C.

VI. SPECTRAL FUNCTION

Now we construct the spectral function for the invariant amplitude (the scalar part of the correlation function) of the tensor glueball current, $\Pi^{\rm QCD}$. The usual lowest resonance plus a continuum model is used to saturate the phenomenological spectral function:

$$\frac{1}{\pi}{\rm Im}\Pi^{\rm PHEN}(s) = \frac{1}{\pi}\rho^{\rm HAD}(s) + \theta(s-s_0)\frac{1}{\pi}{\rm Im}\Pi^{\rm QCD}(s), \quad (44)$$

where s_0 is the QCD-hadron duality threshold, $\theta(s-s_0)$ is the step function, and $\rho^{\rm HAD}(s)$ is the spectral function for the lowest tensor glueball state. In the usual zero-width approximation, the spectral function for a single resonance is assumed to be

$$\rho^{\rm HAD}(s) = F^2\delta(s-m^2), \quad (45)$$

where m is the mass of the lowest glueball, and F is the coupling constant of the current to the glueball defined as

$$\langle 0|O(0)|G\rangle = F. \quad (46)$$

The threshold behavior for $\rho^{\rm HAD}(s)$ is

$$\rho^{\rm HAD}(s) \to \lambda_0^2 s^2\theta(s-4m_\pi^2), \quad \text{for } s\to 4m_\pi^2. \quad (47)$$

In fact, the threshold behavior (47) may only be valid near the chiral limit. Therefore, instead of considering the coupling F as a constant [7], we choose the following model for F:

$$F = \begin{cases} 0, & \text{for } s \le 4m_\pi^2, \\ \lambda_0 s\theta(s-4m_\pi^2), & \text{for } 4m_\pi^2 < s < 4m_\pi^2+\delta s, \\ fm^2, & \text{for } s \ge 4m_\pi^2+\delta s, \end{cases} \quad (48)$$

where λ_0 and f are some constants determined late in the numerical simulation, and δs is a small constant determined by simulation.

To go beyond the zero-width approximation, in facing the near-actual situation, the Breit-Wigner form for a single resonance is assumed for $\rho^{\rm HAD}(s)$,

$$\rho^{\rm HAD}(s) = \frac{F^2 m\Gamma}{(s-m^2+\Gamma^2/4)^2 + m^2\Gamma^2}, \quad (49)$$

where Γ is the width of the lowest glueball. Further, the one-isolated-lowest-resonance assumption is questioned from the admixture with quarkonium states, and it is known from the experimental data that there are three 2^{++} tensor resonances up to and around the mass scale 1.525 GeV. The form of the spectral function for three resonances is taken to be

$$\rho^{\rm HAD}(s) = \sum_{i=1}^{3}\frac{F_i^2 m_i\Gamma_i}{(s-m_i^2+\Gamma_i^2/4)^2 + m_i^2\Gamma_i^2}, \quad (50)$$

where m_i and Γ_i are the mass and width of the ith resonance, respectively. For the sake of simplicity, all coupling constants F_i for $s < m_\pi^2$ are fixed with the same λ_0 as shown in Eq. (48).

VII. FINITE-WIDTH LAPLACIAN SUM RULE

Now we are in a position to construct the appropriate sum rules of the tensor glueball current. The invariant amplitude Π obeys a dispersion relation,

$$\Pi(q^2) = \int_0^\infty ds\frac{1}{s+q^2}\frac{1}{\pi}{\rm Im}\Pi(s) + \text{subtractions}, \quad (51)$$

which is defined up to a finite number n of subtractions. To dispose of the dependence on these subtractions, one takes the nth derivative of $\Pi(q^2)$ to obtain

$$(-1)^n\frac{d^n}{(dQ^2)^n}\Pi(q^2) = \int_0^\infty ds\frac{n!}{(s+Q^2)^{n+1}}\frac{1}{\pi}{\rm Im}\Pi(s), \quad (52)$$

with $Q^2 = q^2$, which can be regarded as a global duality relation (i.e., sum rule) in the sense that the weighted average of the physical spectral function $(1/\pi){\rm Im}\Pi(s) \equiv (1/\pi){\rm Im}\Pi^{\rm PHEN}(s)$ [a model of $(1/\pi){\rm Im}\Pi^{\rm PHEN}(s)$ is given in Eq. (44)], for sufficiently large Q^2 values in the weight, must match the nth derivative of $\Pi(q^2) \equiv \Pi^{\rm QCD}(Q^2)$ on the lhs, which is a calculable quantity in QCD [an approximated form is given in Eq. (43)]. To make the sum rule more sensitive to the low-energy behavior of the spectral function, one applies the Borel transformation

$$\hat{\mathcal{L}} \equiv \lim_{\substack{N\to\infty \\ Q^2\to\infty \\ Q^2/N\equiv t}} \frac{(-1)^N}{(N-1)!}(Q^2)^N\left(\frac{\rm d}{{\rm d}Q^2}\right)^N \quad (53)$$

to both sides of Eq. (52). Then, a family of Laplacian sum rules can be formed [51],

$$\mathcal{L}_k^{\rm HAD}(s_0,t) = \mathcal{L}_k^{\rm QCD}(s_0,t) \quad (54)$$

and

$$\mathcal{L}_k^{\rm HAD}(s_0,t)=\int_0^{s_0} ds s^k e^{-s/t}\frac{1}{\pi}\rho^{\rm HAD}(s), \tag{55}$$

for the phenomenological contributions to the sum rules, and for the theoretical contributions

$$\mathcal{L}_k^{\rm QCD}(s_0,t)=\mathcal{L}_k^{\rm QCD}(t)-\mathcal{L}_k^{\rm CONT}(s_0,t), \tag{56}$$

with $\mathcal{L}_k^{\rm QCD}(t)$ and $\mathcal{L}_k^{\rm CONT}(s_0,t)$ being

$$\mathcal{L}_k^{\rm QCD}(t)=t\hat{\mathcal{L}}[(-Q^2)^k\Pi^{\rm QCD}(Q^2)] \tag{57}$$

and

$$\mathcal{L}_k^{\rm CONT}(s_0,t)=\int_{s_0}^{\infty} ds s^k e^{-s/t}\frac{1}{\pi}{\rm Im}\Pi^{\rm QCD}(s). \tag{58}$$

Substituting Eq. (43) into Eq. (57), we have

$$\begin{aligned}\mathcal{L}_{-1}^{\rm QCD}(t)=&-\overline{n}[c_1\pi\alpha_s^{-1}(t)+c_2\pi\alpha_s^{-1}(t)(t\rho^2)^{-1}\\&+c_3+c_4(t\rho^2)^{-1}-c_5t\rho^2-c_6\gamma\\&+c_7(1-\gamma)(t\rho^2)^{-1}]-a_0t^2,\end{aligned} \tag{59}$$

$$\begin{aligned}\mathcal{L}_0^{\rm QCD}(t)=&\overline{n}[c_2\pi\alpha_s^{-1}(t)\rho^{-2}+c_4\rho^{-2}+c_5t^2\rho^2\\&-c_6t-c_7\gamma\rho^{-2}]-2a_0t^3,\end{aligned} \tag{60}$$

$$\mathcal{L}_1^{\rm QCD}(t)=-\overline{n}(-2c_5\rho^2t^3+c_6t^2-c_7\rho^{-2}t)-6a_0t^4. \tag{61}$$

VIII. NUMERICAL ANALYSIS

The expressions for the three-loop running coupling constant $\alpha_s(Q^2)$ with three massless flavors ($N_f=3$) at the renormalization scale μ [52]

$$\frac{\alpha_s(\mu^2)}{\pi}=\frac{\alpha_s^{(2)}(\mu^2)}{\pi}+\frac{1}{(\beta_0L)^3}\left[L_1\left(\frac{\beta_1}{\beta_0}\right)^2+\frac{\beta_2}{\beta_0}\right] \tag{62}$$

are used, where $\alpha_s^{(2)}(\mu^2)/\pi$ is the two-loop running coupling constant with ($N_f=0$)

$$\frac{\alpha_s^{(2)}(\mu^2)}{\pi}=\frac{1}{\beta_0L}-\frac{\beta_1}{\beta_0}\frac{\ln L}{(\beta_0L)^2} \tag{63}$$

and

$$\begin{aligned}L&=\ln\left(\frac{\mu^2}{\Lambda^2}\right),\\ \beta_0&=\frac{1}{4}\left[11-\frac{2}{3}N_f\right],\\ \beta_1&=\frac{1}{4^2}\left[102-\frac{38}{3}N_f\right],\\ \beta_2&=\frac{1}{4^3}\left[\frac{2857}{2}-\frac{5033}{18}N_f+\frac{325}{54}N_f^2\right],\end{aligned} \tag{64}$$

with the color number $N_c=3$ and the QCD renormalization invariant scale $\Lambda=120$ MeV. We take $\mu^2=t$ after calculating Borel transforms based on the renormalization group improvement for Laplacian sum rules [53]. The values of the average instanton size and the overall instanton density are adopted from the instanton liquid model [29],

$$\begin{aligned}\overline{n}&=1\ {\rm fm}^{-4}=0.0016\ {\rm GeV}^4,\\ \overline{\rho}&=\frac{1}{3}{\rm fm}\simeq 1.667\ {\rm GeV}^{-1}.\end{aligned} \tag{65}$$

The resonance masses and widths appearing in Eq. (50) could be estimated by optimally matching both sides of the sum rules (55) in the fiducial domain (sum rule window) where the mentioned resonance parameters should be approximately stable. At $t_{\rm max}$ of the sum rule window, the resonance contribution should be greater than the continuum one,

$$\mathcal{L}_k^{\rm QCD}(s_0,t_{\rm max})\geq\mathcal{L}_k^{\rm CONT}(s_0,t_{\rm max}), \tag{66}$$

according to the standard requirement that in the energy region above $t_{\rm max}$ the perturbative contribution is dominant. At $t_{\rm min}$, which lies in the low-energy region, we require that the single instanton contribution should be relatively large so that

$$\frac{\mathcal{L}_k^{\rm int}(s_0,t_{\rm min})}{\mathcal{L}_k^{\rm QCD}(s_0,t_{\rm min})}\geq 50\%. \tag{67}$$

At the same time, to keep the multi-instanton correction negligible, we simply adopt the rough estimate

$$t_{\rm min}\geq(2\overline{\rho})^{-2}\sim\left(\frac{2}{0.6\ {\rm GeV}}\right)^{-2}. \tag{68}$$

To determine the value s_0 for the threshold, it is obvious that s_0 must be greater than the squared masses of all of the considered resonances, and should guarantee that there is a sum rule window for the stability of our Laplacian sum rules. According to the above requirements, we find that in the domain

$$t\in(1.0,3.0)\ {\rm GeV}^2,\qquad s_0\in(2.9,3.9)\ {\rm GeV}^2 \tag{69}$$

our sum rules work very well for, e.g., $k=-1, 0, 1$, as usual, to consider the very important information comes from the low-energy theorem. Finally, in order to measure the compatibility between both sides of the sum rules (55) in our numerical simulation, we divide the sum rule window $[t_{\rm min},t_{\rm max}]$ into $N=100$ segments of equal width, $[t_i,t_{i+1}]$, with $t_0=t_{\rm min}$ and $t_N=t_{\rm max}$, and introduce a variation δ which is defined as

TABLE I. The optimal fitting values of the mass m, width Γ, coupling constant f, continuum threshold s_0, and compatibility measure δ for the possible 2^{++} resonances in the sum rule window $[t_{\min}, t_{\max}]$ for the best matching between the lhs and rhs of the sum rules (55) with $k = -1, 0, 1$ are listed, while all of the pure perturbative and interference contributions are included in the correlation function for cases A, B, and C, in which a single zero-width resonance plus the continuum model of the spectral function is adopted for case A, a single finite-width resonance plus the continuum model is adopted for case B, and three finite-width resonances plus the continuum model is adopted for case C.

Cases	k	Resonances	m (GeV)	Γ (GeV)	f (GeV)	$s_0(\mathrm{GeV}^2)$	$[t_{\min}, t_{\max}](\mathrm{GeV}^2)$	δ
	-1		1.520	0	0.140	3.9	1.0–3.0	3.4×10^{-4}
A	0	Glueball	1.523	0	0.112	3.3	1.0–3.0	8.4×10^{-5}
	1		1.521	0	0.094	3.0	1.0–3.0	4.9×10^{-5}
	-1		1.525	0.105	0.058	3.1	1.0–3.0	4.3×10^{-5}
B	0	Glueball	1.525	0.110	0.059	3.1	1.0–3.0	1.8×10^{-4}
	1		1.525	0.097	0.052	2.9	1.0–3.0	8.3×10^{-5}
		$f_2(1270)$	1.275	0.185	0.022			
	-1	$f_2'(1525)$	1.525	0.073	0.052	3.0	1.0–3.0	4.4×10^{-5}
		$f_2(1950)$	1.944	0.472	0.010			
		$f_2(1270)$	1.275	0.185	0.010			
C	0	$f_2'(1525)$	1.525	0.073	0.050	3.0	1.0–3.0	4.1×10^{-5}
		$f_2(1950)$	1.944	0.472	0.028			
		$f_2(1270)$	1.275	0.185	0.010			
	1	$f_2'(1525)$	1.525	0.073	0.054	3.0	1.0–3.0	1.4×10^{-4}
		$f_2(1950)$	1.944	0.472	0.010			

$$\delta = \frac{1}{N}\sum_{i=1}^{N}\frac{[L(t_i) - R(t_i)]^2}{|L(t_i)R(t_i)|}, \tag{70}$$

where $L(t_i)$ and $R(t_i)$ are the lhs and rhs of Eq. (55) evaluated at t_i.

Let us first consider the case of single-resonance-plus-continuum models [specified by Eqs. (46) and (50), respectively] for the spectral function. The optimal parameters governing the sum rules with zero and finite widths are listed in the first six lines of Table I and the corresponding curves for the lhs and rhs of Eq. (55) with $k = -1$, 0, and $+1$ are displayed in Figs. 2 and 3, respectively. From Table I, the optical values of the tensor glueball mass, width, coupling, and duality threshold with the best matching are

$$\begin{aligned} m &= 1.522 \pm 0.002\ \mathrm{GeV}, \\ f &= 0.115 \pm 0.025\ \mathrm{GeV}, \\ s_0 &= 3.4 \pm 0.5\ \mathrm{GeV}^2 \end{aligned} \tag{71}$$

for one zero-width resonance model, and

$$\begin{aligned} m &= 1.525\ \mathrm{GeV}, \\ \Gamma &= 0.104 \pm 0.007\ \mathrm{GeV}, \\ f &= 0.055 \pm 0.004\ \mathrm{GeV}, \\ s_0 &= 3.0 \pm 0.1\ \mathrm{GeV}^2 \end{aligned} \tag{72}$$

for one finite-width resonance model, where here and hereafter the errors are estimated from the uncertainties of the spread between the individual sum rules. For the case of three finite-width resonances plus the continuum model (50) for the spectral function, the optimal parameters governing the sum rules are listed in the remaining lines of Table I. The corresponding curves for the lhs and rhs of Eq. (55) with $k = -1$, 0, and $+1$ are displayed in Fig. 4. Taking the average, the optical values of the widths of the three lowest 2^{++} resonances in the world of QCD with three massless quarks and the corresponding optical fit parameters are predicted to be

$$\begin{aligned} m_{f_2(1270)} &= 1.275\ \mathrm{GeV}, \\ f_{f_2(1270)} &= 0.016 \pm 0.006\ \mathrm{GeV}, \\ \Gamma_{f_2(1270)} &= 0.185\ \mathrm{GeV}, \end{aligned} \tag{73}$$

$$\begin{aligned} m_{f_2'(1525)} &= 1.525\ \mathrm{GeV}, \\ f_{f_2'(1525)} &= 0.052 \pm 0.002\ \mathrm{GeV}, \\ \Gamma_{f_2'(1525)} &= 0.073\ \mathrm{GeV}, \end{aligned} \tag{74}$$

$$\begin{aligned} m_{f_2(1950)} &= 1.944\ \mathrm{GeV}, \\ f_{f_2(1950)} &= 0.019 \pm 0.009\ \mathrm{GeV}, \\ \Gamma_{f_2(1950)} &= 0.472\ \mathrm{GeV}, \end{aligned} \tag{75}$$

with

$$s_0 = 3.0\ \mathrm{GeV}. \tag{76}$$

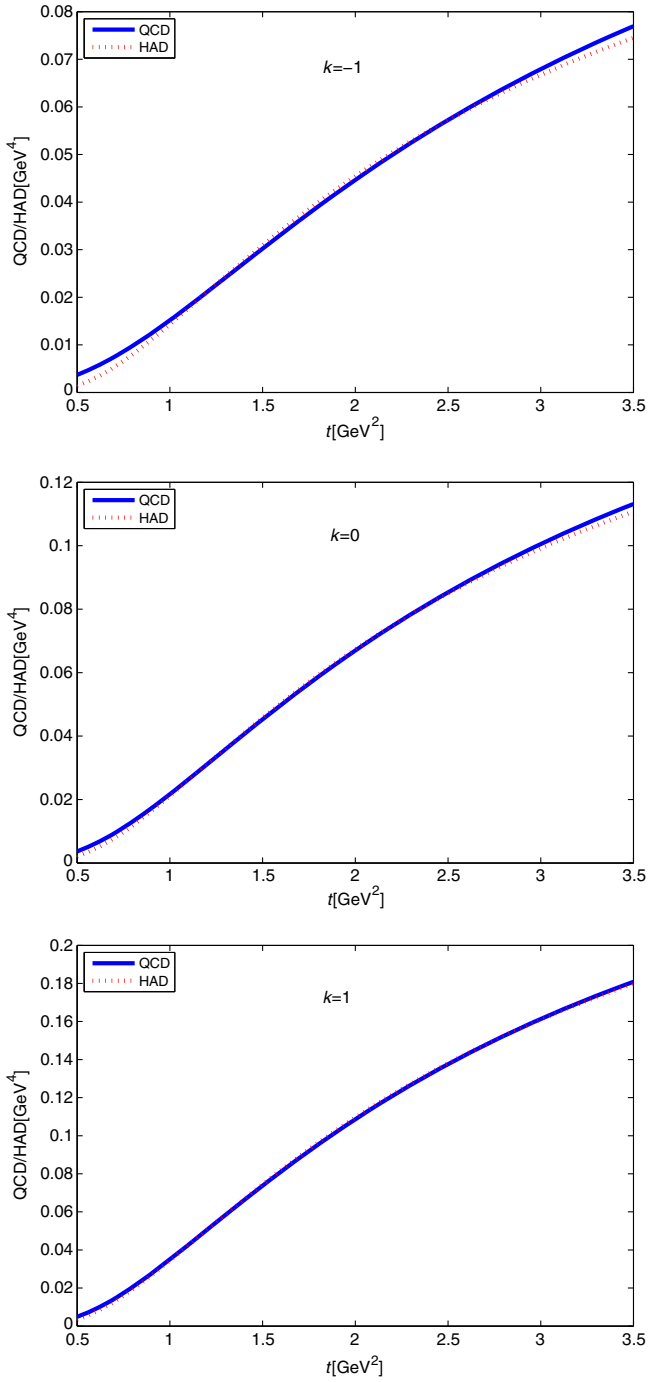

FIG. 2. The lhs (dot line) and rhs (solid line) of the sum rules (55) with $k = -1$, 0, 1 versus t in the case where the correlation function Π^{QCD} contains the interference and pure perturbative contributions, and a single zero-width resonance plus the continuum model is adopted for the spectral function.

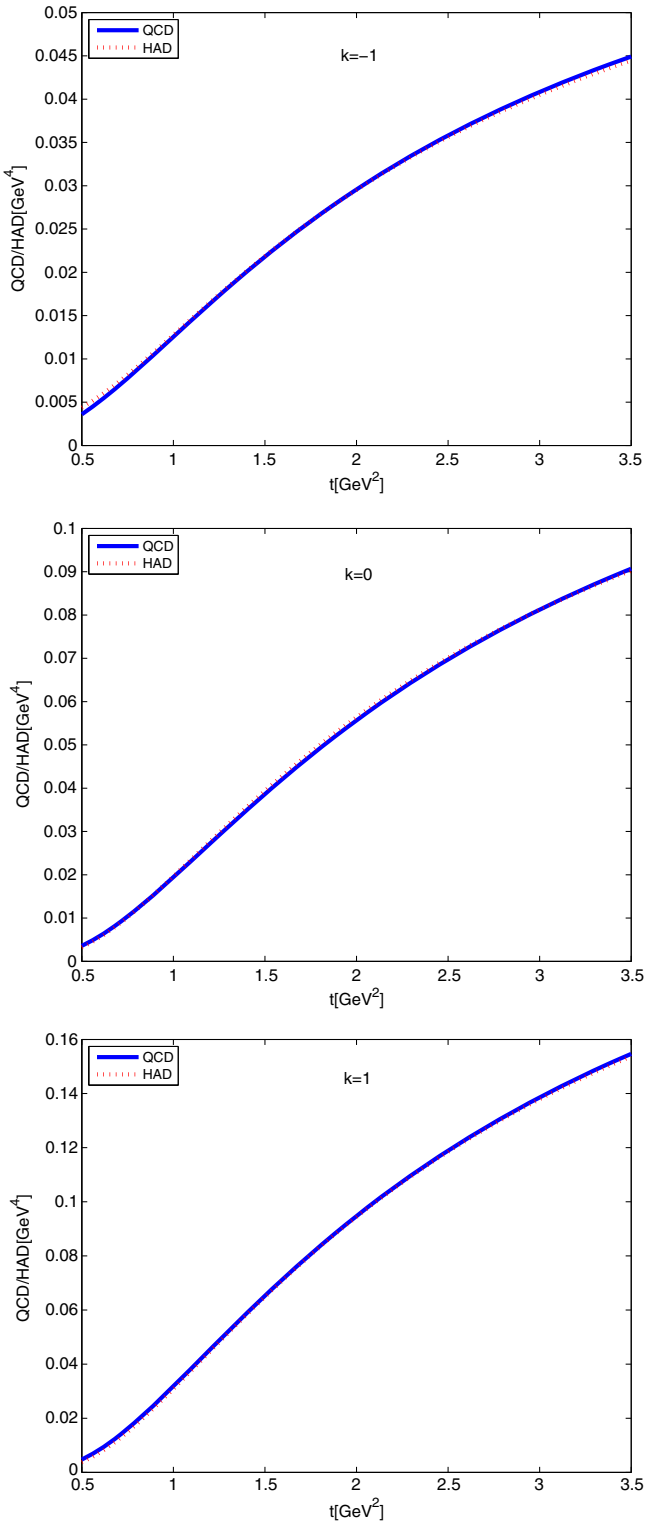

FIG. 3. The lhs (dashed line) and rhs (solid line) of the sum rules (55) with $k = -1$, 0, 1 versus t in the case where the correlation function Π^{QCD} contains the interference and pure perturbative contributions, and a single finite-width resonance plus the continuum model is adopted for the spectral function.

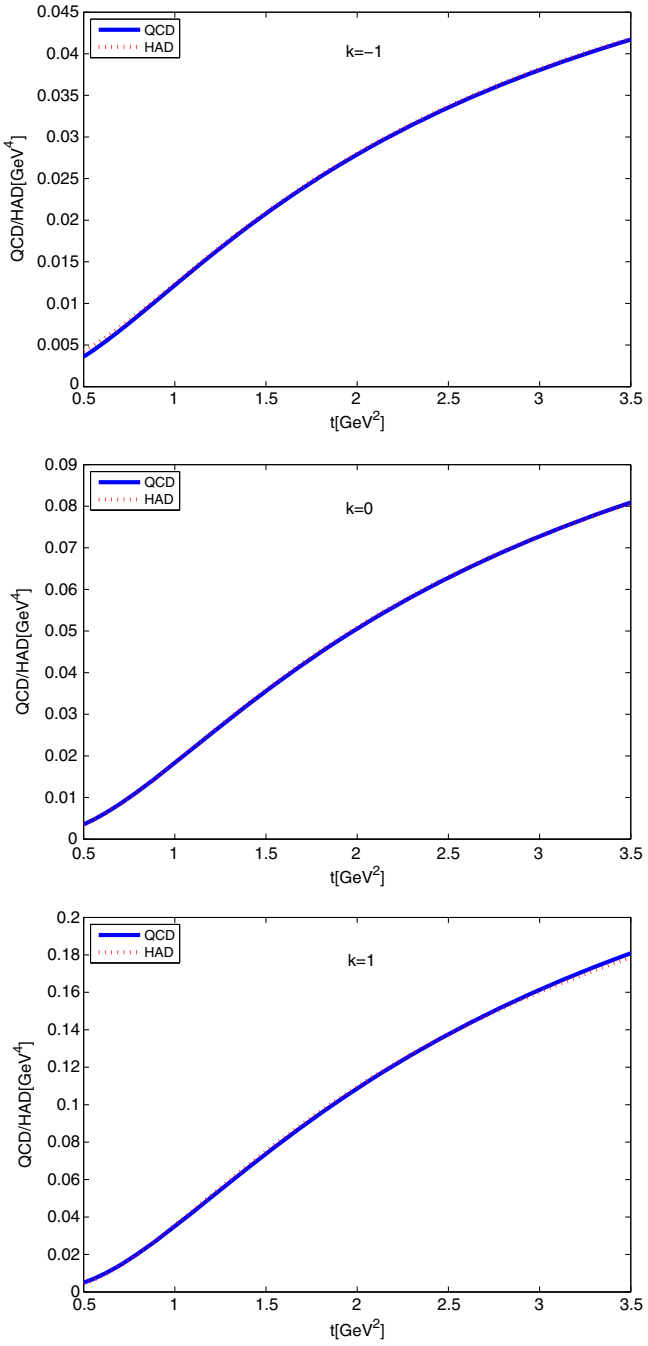

FIG. 4. The lhs (dashed line) and rhs (solid line) of the sum rules (55) with $k=-1$, 0, 1 versus t in the case where the correlation function Π^{QCD} contains the interference and pure perturbative contributions, and a three-finite-width-resonances-plus-continuum model is adopted for the spectral function.

IX. CONCLUSION AND DISCUSSION

The main results of this work can be summarized as follows.

First, the contribution to the correlation function arising from the interference between the classical instanton fields and the quantum gluon ones was derived in the framework of the semiclassical expansion of the instanton liquid vacuum model of QCD. The resultant expression is gauge invariant, and free of the infrared divergence. It plays a great role in sum-rule analysis in accordance with the spirit of the semiclassical expansion. The imaginary part of the correlation function including this interference contribution is positive, as shown in Fig. 6 in Appendix D. Moreover, the traditional condensate contribution is excluded in the correlation function to avoid double counting [7], because condensates can be reproduced by the instanton distributions [29–32]. Another reason to do so is that the usual condensate contribution is proven to be unusually weak, and cannot fully reflect the nonperturbative nature of the low-lying gluonia [7,15,16,54]; in our opinion, the condensate contribution may be considered as a small fraction of the corresponding instanton one, so it is naturally taken into account already.

Second, the properties of the lowest-lying 2^{++} tensor glueball were systematically investigated in a family of Laplacian sum rules in three different cases: a single zero-width resonance plus the continuum model of the spectral function was adopted for case A, a single finite-width resonances plus the continuum model was adopted for case B, and the three finite-width resonances plus the continuum model was adopted for case C. The optimal fitting values of the mass m, width Γ, coupling constant f, and continuum threshold s_0 for the possible 2^{++} resonances were obtained, and are quite consistent with each other. The resultant Laplacian sum rules with $k=-1,0,+1$ were carried out with a few of the standard QCD input parameters, in accordance with the experimental data.

Let us now identify where the lowest-lying 2^{++} tensor glueball is located. The results for the single-resonance-plus-continuum models A and B [namely, Eqs. (70) and (72)] imply that the meson $f_2'(1525)$ may be the most viable candidate for the lowest-lying 2^{++} tensor glueball because the difference between the two models is just the width of the resonances, and the latter is of course believed to be more in accordance with reality. This conclusion can further be justified by the result of the three-resonances-plus-continuum model [namely, Eqs. (73), (74), and (75)], which shows that $f_{f_2'(1525)}$ is dominant.

As a discussion, we compare our result with other works. Let us mention the following points in order.

(a) The results from lattice QCD are extracted from the fit equation (2) in Ref. [55] by the variational procedure in Monte Carlo simulations [36]; however, the mass of the lowest-lying glueball should be understood as the upper bound of the glueball in the channel of interest. It is important to note that our result in this work is estimated from the match both sides of our sum rule, and should be compared to reality; in the sense of an

upper bound on the mass, our result is consistent with those of lattice QCD.

(b) The so-called mass hierarchy [56] for the lowest 0^{++}, 2^{++}, and 0^{-+} glueballs (namely, $m_{0^{++}} < m_{2^{++}} < m_{0^{-+}}$) comes from lattice QCD; it is difficult to understand because it is, in fact, an inequality of the possible upper bounds on the mass determined by the variational principle. On the other hand, phenomenologically, the identification of the pseudoscalar glueball has been a matter of debate since the Mark II experiment proposed glueball candidates [57]. Later, in the mass region of the first radial excitation of the η and η' mesons, a supernumerous candidate—the $\eta(1405)$—was observed. It seems to be clear that $\eta(1405)$ is allowed as a glueball-dominated state mixed with isoscalar $q\bar{q}$ states due to its behavior in production and decays, namely, it has comparably large branching ratios in the J/ψ radiative decay, but it has not been observed in $\gamma\gamma$ collisions [19,55,58]. A review of the experimental status of $q\bar{q}$ was given in Ref. [19]. However, this state lies considerably lower than the theoretical expectations: the lattice QCD predictions suggest a glueball around 2.5 GeV [36,59]; the mass scale of the pseudoscalar glueball obtained in the QCD sum rule approach is above 2 GeV [7,15,16,60]. Moreover, there are attractive arguments for the scalar and pseudoscalar glueballs being approximately degenerate in mass [61], and even the scenario that a pseudoscalar glueball may be lower in mass than the scalar one was recently discussed in Ref. [62]. The possibly nonvanishing gluonium content of the ground state η and η' mesons was discussed in Refs. [12,63–65]. Up to now, only the topological model of the glueball as a closed flux tube [61] predicts a degeneracy of the 0^{++} and 0^{-+} glueball masses and admits the region 1.3–1.5 GeV before our recent result [13,14,17,18] was published.

(c) The results in QCD-based constituent models are inconsistent and even contradictory with each other: the lowest-lying 2^{++} glueball lies in the mass region 0.96–2.5 GeV [55], and our prediction is located in between.

(d) In the QCD sum rule approach, our result is higher than the previous one ($\approx$1.26 GeV) from Refs. [66,67], and lower than the other ones ($\approx$2.0 GeV) [40,41].

(e) We note here that a recent phenomenological analysis [68] predicted that the mass of the lowest-lying tensor glueball 1.40 ± 0.14 GeV, which is close to, but lower than our present result.

(f) Finally, it is important to note that the Laplacian sun rule (54) is based on the Borel transform for the global duality relation (52), and not based on the so-called strict local duality

$$\frac{1}{\pi}\Pi^{\mathrm{QCD}}(s) = \frac{1}{\pi}\Pi^{\mathrm{PHEN}}(s), \tag{77}$$

which corresponds the Gauss-Weierstrass transformed sum rule in an appropriate limit [51]. This limit would be equivalent to knowing the spectral function everywhere, as well as the full perturbative and nonperturbative dynamical effects of QCD; however, it is an impossible task given the present state of development of QCD and the experiments. We note here that by integrating both sides of Eq. (77) from $s = 0$ to $s = s_0$, we get the so-called finite-energy sum rule

$$\int_0^{s_0} ds \frac{1}{\pi}\Pi^{\mathrm{QCD}}(s) = \int_0^{s_0} ds \frac{1}{\pi}\Pi^{\mathrm{PHEN}}(s), \tag{78}$$

which is usually used to determine the approximate value of the threshold s_0 in the sum rule. The lhs and rhs of Eq. (78), as functions of s_0, are shown in Fig. 7 in Appendix E, where the abscissa of the intersection point of the two curves gives the value of s_0, which is very close to that given in Eq. (76).

In summary, our results suggest that $f_2'(1525)$ is a good candidate for the lowest 2^{++} tensor glueball with some mixture with the nearby excited isovector and isoscalar $q\bar{q}$ mesons. The predicted mass of the lowest-lying tensor glueball is only a little bit higher than that of the scalar one (1500 MeV) determined recently according to the same approach [14]. The reason may be that, although the leading instanton contribution is absent from the tensor channel of glueballs, there is still a strong attractive force arising from the interference between the quantum gluon fields and the classical one, which almost solely governs the final result. Such a situation is somehow the same as in the case of the scalar channel, which causes the lowest scalar and tensor glueballs to be almost degenerate, just as predicted in the conventional bag model. The small difference between the masses of the glueball states could be understood as the spin splitting. To explore the deep physical reason for the above points, further investigation will certainly be needed.

ACKNOWLEDGMENTS

This work is supported by the BEPC National Laboratory Project of Research and Development and the BES Collaboration Research Foundation.

APPENDIX A: THE OPERATORS $\tilde{O}_{\mu\nu}{}^{(i)}$

The operators $\tilde{O}_{\mu\nu}{}^{(i)}$ in terms of instanton and quantum gluon fields are

$$
\begin{aligned}
\tilde{O}^{(1)}_{\mu\nu} &= F_{a\mu\rho}F_{a\nu\rho},\\
\tilde{O}^{(2)}_{\mu\nu} &= F_{a\phi\rho}a_{b\beta,\alpha}\delta_{ab}(\delta_{\alpha\varphi}\delta_{\beta\rho}-\delta_{\alpha\rho}\delta_{\beta\varphi})(\delta_{\varphi\mu}\delta_{\phi\nu}+\delta_{\varphi\nu}\delta_{\phi\mu}),\\
\tilde{O}^{(3)}_{\mu\nu} &= g_sF_{a\phi\rho}A_{c\alpha}a_{b\beta}f_{acb}(\delta_{\alpha\varphi}\delta_{\beta\rho}-\delta_{\alpha\rho}\delta_{\beta\varphi})\\
&\quad\times(\delta_{\varphi\mu}\delta_{\phi\nu}+\delta_{\varphi\nu}\delta_{\phi\mu}),\\
\tilde{O}^{(4)}_{\mu\nu} &= a_{b\beta,\alpha}a_{d\lambda,\kappa}\delta_{ab}\delta_{ad}(\delta_{\alpha\mu}\delta_{\beta\rho}-\delta_{\alpha\rho}\delta_{\beta\mu})(\delta_{\kappa\nu}\delta_{\lambda\rho}-\delta_{\kappa\rho}\delta_{\lambda\nu}),\\
\tilde{O}^{(5)}_{\mu\nu} &= g_s(A_{e\kappa}a_{d\lambda}a_{b\beta,\alpha}f_{aed}\delta_{ab}+A_{c\alpha}a_{b\beta}a_{d\lambda,\kappa}f_{acb}\delta_{ad})\\
&\quad\times(\delta_{\alpha\mu}\delta_{\beta\rho}-\delta_{\alpha\rho}\delta_{\beta\mu})(\delta_{\kappa\nu}\delta_{\lambda\rho}-\delta_{\kappa\rho}\delta_{\lambda\nu}),\\
\tilde{O}^{(6)}_{\mu\nu} &= g_s^2A_{c\alpha}A_{e\kappa}a_{b\beta}a_{d\lambda}f_{acb}f_{aed}(\delta_{\alpha\mu}\delta_{\beta\rho}-\delta_{\alpha\rho}\delta_{\beta\mu})\\
&\quad\times(\delta_{\kappa\nu}\delta_{\lambda\rho}-\delta_{\kappa\rho}\delta_{\lambda\nu}),\\
\tilde{O}^{(7)}_{\mu\nu} &= g_sF_{a\phi\lambda}a_{b\beta}a_{d\lambda}f_{abd}\delta_{\beta\varphi}(\delta_{\varphi\mu}\delta_{\phi\nu}+\delta_{\varphi\nu}\delta_{\phi\mu}),\\
\tilde{O}^{(8)}_{\mu\nu} &= g_sa_{d\nu}a_{e\rho}a_{b\beta,\alpha}f_{ade}\delta_{ab}(\delta_{\alpha\mu}\delta_{\beta\rho}-\delta_{\alpha\rho}\delta_{\beta\mu})\\
&\quad+g_sa_{b\mu}a_{c\rho}a_{d\lambda,\kappa}f_{abc}\delta_{ad}(\delta_{\kappa\nu}\delta_{\lambda\rho}-\delta_{\kappa\rho}\delta_{\lambda\nu}),\\
\tilde{O}^{(9)}_{\mu\nu} &= g_s^2f_{acb}f_{ade}A_{c\alpha}a_{b\beta}a_{d\nu}a_{e\rho}(\delta_{\alpha\mu}\delta_{\beta\rho}-\delta_{\alpha\rho}\delta_{\beta\mu})\\
&\quad+g_s^2f_{acb}f_{ade}A_{e\kappa}a_{b\mu}a_{c\rho}a_{d\lambda}(\delta_{\kappa\nu}\delta_{\lambda\rho}-\delta_{\kappa\rho}\delta_{\lambda\nu}),\\
\tilde{O}^{(10)}_{\mu\nu} &= g_s^2a_{b\mu}a_{c\rho}a_{d\nu}a_{e\rho}f_{abc}f_{ade},
\end{aligned}
\tag{A1}
$$

where $F_{a\mu\nu}$ is the instanton field strength associated with the instanton field A.

APPENDIX B: THE INTERFERENCE CONTRIBUTIONS $\Pi_i^{(\mathrm{int})}$ IN TERMS OF THE OPERATORS $\tilde{O}_{\mu\nu}{}^{(i)}$

The expressions for $\Pi_i^{(\mathrm{int})}$ in terms of $\tilde{O}^{(i)}_{\mu\nu}$ are

$$
\begin{aligned}
\Pi_1^{(\mathrm{int})} &= \hat{T}\langle\Omega|T\tilde{O}^{(2)}_{\mu\nu}(x)\tilde{O}^{(2)}_{\mu'\nu'}(0)|\Omega\rangle,\\
\Pi_2^{(\mathrm{int})} &= 2\hat{T}\langle\Omega|T\tilde{O}^{(2)}_{\mu\nu}(x)\tilde{O}^{(3)}_{\mu'\nu'}(0)|\Omega\rangle,\\
\Pi_3^{(\mathrm{int})} &= \hat{T}\langle\Omega|T\tilde{O}^{(3)}_{\mu\nu}(x)\tilde{O}^{(3)}_{\mu'\nu'}(0)|\Omega\rangle,\\
\Pi_4^{(\mathrm{int})} &= 2\hat{T}\langle\Omega|T\tilde{O}^{(4)}_{\mu\nu}(x)\tilde{O}^{(5)}_{\mu'\nu'}(0)|\Omega\rangle,\\
\Pi_5^{(\mathrm{int})} &= 2\hat{T}\langle\Omega|T\tilde{O}^{(4)}_{\mu\nu}(x)\tilde{O}^{(6)}_{\mu'\nu'}(0)|\Omega\rangle,\\
\Pi_6^{(\mathrm{int})} &= 2\hat{T}\langle\Omega|T\tilde{O}^{(4)}_{\mu\nu}(x)\tilde{O}^{(7)}_{\mu'\nu'}(0)|\Omega\rangle,\\
\Pi_7^{(\mathrm{int})} &= \hat{T}\langle\Omega|T\tilde{O}^{(5)}_{\mu\nu}(x)\tilde{O}^{(5)}_{\mu'\nu'}(0)|\Omega\rangle,\\
\Pi_8^{(\mathrm{int})} &= \hat{T}\langle\Omega|T\tilde{O}^{(7)}_{\mu\nu}(x)\tilde{O}^{(7)}_{\mu'\nu'}(0)|\Omega\rangle,\\
\Pi_9^{(\mathrm{int})} &= 2\hat{T}\langle\Omega|T\tilde{O}^{(5)}_{\mu\nu}(x)\tilde{O}^{(7)}_{\mu'\nu'}(0)|\Omega\rangle,\\
\Pi_{10}^{(\mathrm{int})} &= 2\hat{T}\langle\Omega|T\tilde{O}^{(6)}_{\mu\nu}(x)\tilde{O}^{(7)}_{\mu'\nu'}(0)|\Omega\rangle,\\
\Pi_{11}^{(\mathrm{int})} &= 2\hat{T}\langle\Omega|T\tilde{O}^{(5)}_{\mu\nu}(x)\tilde{O}^{(6)}_{\mu'\nu'}(0)|\Omega\rangle,\\
\Pi_{12}^{(\mathrm{int})} &= \hat{T}\langle\Omega|T\tilde{O}^{(6)}_{\mu\nu}(x)\tilde{O}^{(6)}_{\mu'\nu'}(0)|\Omega\rangle,
\end{aligned}
\tag{B1}
$$

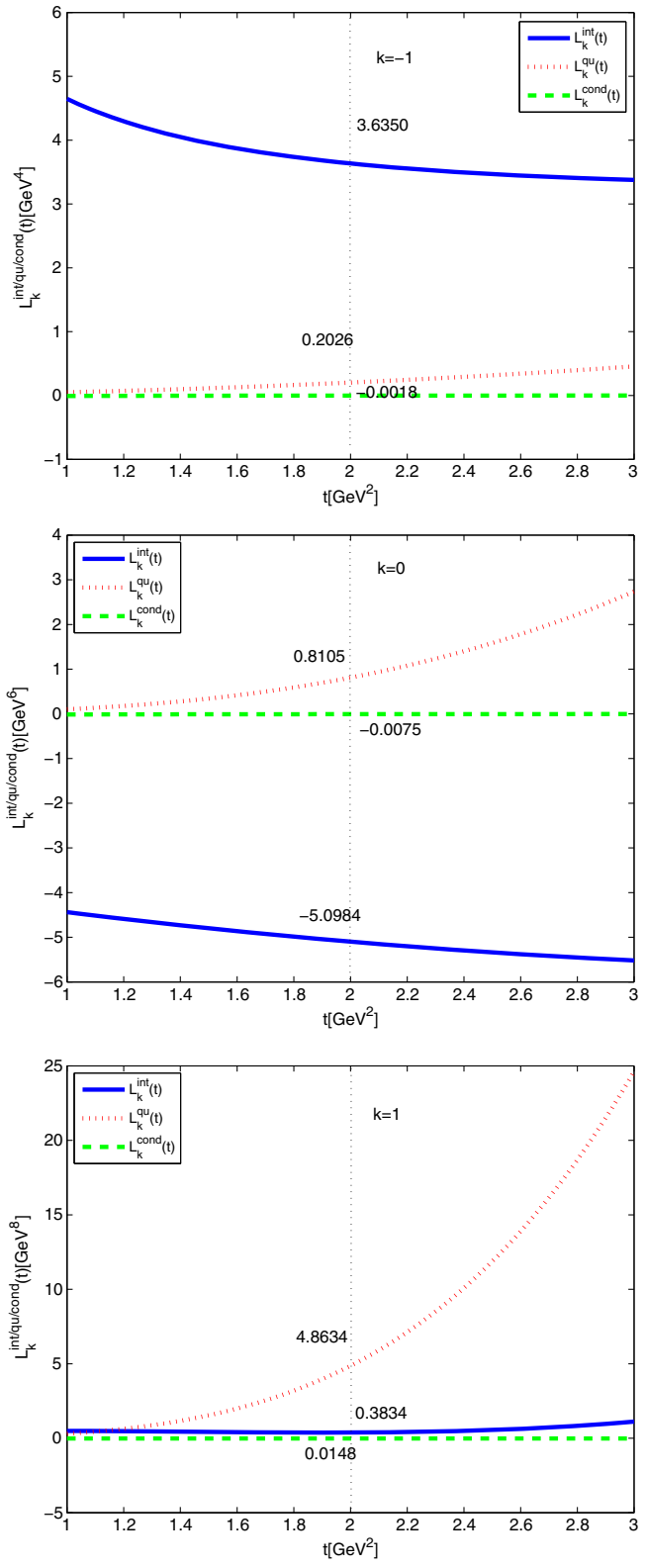

FIG. 5. The magnitudes of the Borel transformations of $\Pi^{(\mathrm{int})}$ (solid line), $\Pi^{(\mathrm{qu})}$ (dotted line), and $\Pi^{(\mathrm{cond})}$ (dashed line) with $k=-1$, 0, 1 versus t.

where

$$\hat{T} \equiv 2\overline{n}\left(\delta_{\mu\mu'}\delta_{\nu\nu'} - \frac{1}{4}\delta_{\mu\nu}\delta_{\mu'\nu'}\right)\int d^4z \int d^4x e^{iq\cdot x}. \quad \text{(B2)}$$

APPENDIX C: THE BOREL TRANSFORM OF THE CONDENSATE CONTRIBUTION

Substituting Eq. (29) into Eq. (57), we obtain the expression for the Borel transformation of the condensate contribution as follows:

$$\mathcal{L}_{-1}^{\text{cond}}(t) = \frac{1}{2t^2}\frac{50\pi\alpha_s}{3}\langle 2O_1 - O_2\rangle, \quad \text{(C1)}$$

$$\mathcal{L}_{0}^{\text{cond}}(t) = \frac{1}{t}\frac{50\pi\alpha_s}{3}\langle 2O_1 - O_2\rangle, \quad \text{(C2)}$$

$$\mathcal{L}_{1}^{\text{cond}}(t) = \frac{50\pi\alpha_s}{3}\langle 2O_1 - O_2\rangle. \quad \text{(C3)}$$

The comparison of $\mathcal{L}^{\text{cond}}$ with the other Borel-transformed contributions is shown in Fig. 5.

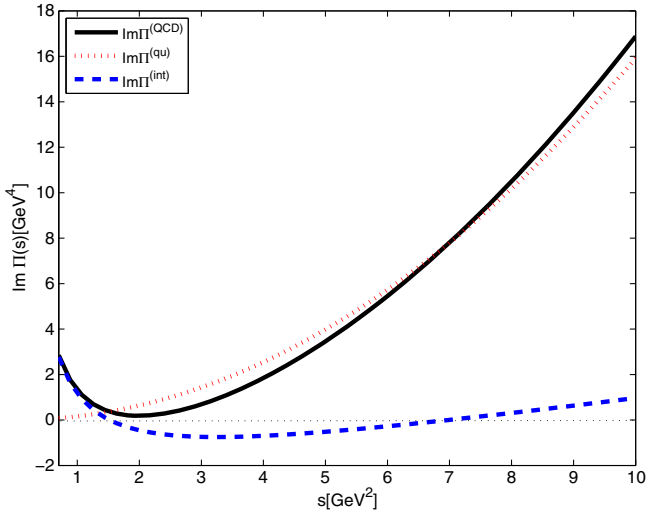

FIG. 6. The contributions to the imaginary parts of the correlation function from the interference (dashed line), pure perturbative (dotted line), and total contribution (solid line) versus s.

APPENDIX D: THE IMAGINARY PARTS OF THE INIERFERENCE AND PERTURBATION CONTRIBUTIONS

The imaginary part of the correlation function from the interference contribution is

$$\text{Im}\Pi^{(\text{int})} = \overline{n}[c_5\rho^2 s - c_6 + c_7(s\rho^2)^{-1}], \quad \text{(D1)}$$

and the one from the pure perturbative contribution is

$$\text{Im}\Pi^{(\text{qu})} = \frac{s^2}{2\pi}. \quad \text{(D2)}$$

Both contributions are shown in Fig. 6.

APPENDIX E: DETERMINATION OF THE THRESHOLD s_0 FROM THE FINITE-ENERGY SUM RULE

The finite-energy sum rule for determining the value of the threshold s_0 reads

$$\int_0^{s_0} ds\frac{1}{\pi}\Pi^{\text{QCD}}(s) = \int_0^{s_0} ds\frac{1}{\pi}\rho^{\text{HAD}}(s). \quad \text{(E1)}$$

The lhs and rhs of Eq. (E1) versus s_0 are plotted as the solid and dotted curves, respectively, in Fig. 7, and the abscissa of the intersection point of the two curves is $s_0 = 2.98\ \text{GeV}^2$, as indicated in the figure.

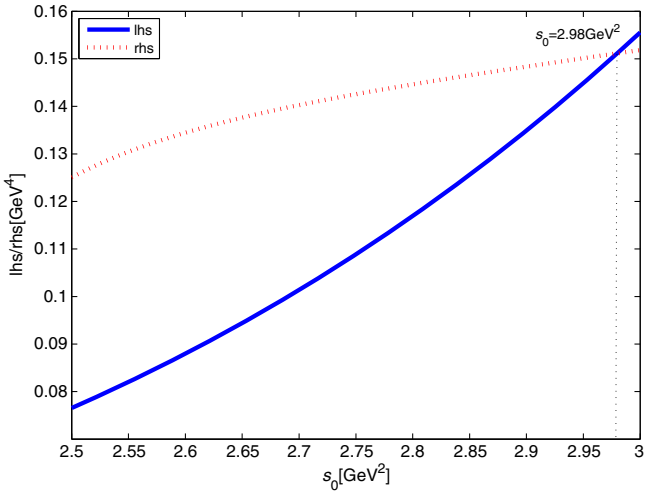

FIG. 7. The lhs (solid line) and rhs (dotted line) of Eq. (E1) versus s_0.

[1] A. Patel, R. Gupta, G. Guralnik, G. W. Kilcup, and S. R. Sharpe, Phys. Rev. Lett. **57**, 1288 (1986).
[2] A. Vaccarino and D. Weingarten, Phys. Rev. D **60**, 114501 (1999).
[3] X.-F. Meng, G. Li, Y.-J. Zhang, Y. Chen, C. Liu, Y.-B. Liu, J.-P. Ma, and J.-B. Zhang, Phys. Rev. D **80**, 114502 (2009).
[4] N. Isgur, R. Kokoski, and J. E. Paton, Phys. Rev. Lett. **54**, 869 (1985).
[5] A. Anisovich, V. Anisovich, and A. Sarantsev, Phys. Lett. B **395**, 123 (1997).
[6] M. Albaladejo and J. Oller, Phys. Rev. Lett. **101**, 252002 (2008).
[7] H. Forkel, Phys. Rev. D **71**, 054008 (2005).
[8] J.-P. Liu and D.-H. Liu, J. Phys. G **19**, 373 (1993).
[9] T. Schäfer and E. V. Shuryak, Phys. Rev. Lett. **75**, 1707 (1995).
[10] L. S. Kisslinger and M. B. Johnson, Phys. Lett. B **523**, 127 (2001).
[11] D. Harnett and T. G. Steele, Nucl. Phys. **A695**, 205 (2001).
[12] H.-Y. Cheng, H.-n. Li, and K.-F. Liu, Phys. Rev. D **79**, 014024 (2009).
[13] S. Wen, Z. Zhang, and J. Liu, Phys. Rev. D **82**, 016003 (2010).
[14] S. Wen, Z. Zhang, and J. Liu, J. Phys. G **38**, 015005 (2011).
[15] C. Xian, F. Wang, and J. Liu, J. Phys. G **41**, 035004 (2014).
[16] C. Xian, F. Wang, and J. Liu, Eur. Phys. J. Plus **128**, 115 (2013).
[17] F. Wang, J. Chen, and J. Liu, Phys. Rev. D **92**, 076004 (2015).
[18] F. Wang, J. Chen, and J. Liu, Eur. Phys. J. C **75**, 460 (2015).
[19] A. Masoni, C. Cicalo, and G. Usai, J. Phys. G **32**, R293 (2006).
[20] V. Crede and C. Meyer, Prog. Part. Nucl. Phys. **63**, 74 (2009).
[21] G. 't Hooft, Phys. Rev. D **14**, 3432 (1976).
[22] T. Schäfer and E. V. Shuryak, Rev. Mod. Phys. **70**, 323 (1998).
[23] V. Vento, Phys. Rev. D **73**, 054006 (2006).
[24] D. Diakonov, Prog. Part. Nucl. Phys. **51**, 173 (2003).
[25] E. V. Shuryak, *Continuous Advances in QCD 2006* (World Scientific, 2012), pp. 3–16.
[26] E.-M. Ilgenfritz and M. Muller-Preussker, Nucl. Phys. **B184**, 443 (1981).
[27] D. Diakonov and V. Y. Petrov, Nucl. Phys. **B245**, 259 (1984).
[28] D. Diakonov and V. Y. Petrov, Nucl. Phys. **B272**, 457 (1986).
[29] E. V. Shuryak, Nucl. Phys. **B203**, 116 (1982).
[30] D. Diakonov and V. Y. Petrov, Phys. Lett. **147B**, 351 (1984).
[31] C. Edwards and *et al.*, Phys. Rev. Lett. **49**, 259 (1982).
[32] J.-P. Liu and P.-X. Yang, J. Phys. G **21**, 751 (1995).
[33] H. Forkel, Phys. Rev. D **64**, 034015 (2001).
[34] Z. Zhang and J. Liu, Chin. Phys. Lett. **23**, 2920 (2006).
[35] J. Cornwall and A. Soni, Phys. Lett. **120B**, 431 (1983).
[36] C. J. Morningstar and M. Peardon, Phys. Rev. D **60**, 034509 (1999).
[37] F. Niedermayer, P. Rfenacht, and U. Wenger, Nucl. Phys. **B597**, 413 (2001).
[38] V. Novikov, M. Shifman, A. Vainshtein, and V. Zakharov, Nucl. Phys. **B174**, 378 (1980).
[39] V. Novikov, M. A. Shifman, A. Vainshtein, and V. I. Zakharov, Nucl. Phys. **B191**, 301 (1981).
[40] S. Narison, Nucl. Phys. **B509**, 312 (1998).
[41] S. Narison, Nucl. Phys. **A675**, 54 (2000).
[42] N. Isgur and J. Paton, Phys. Rev. D **31**, 2910 (1985).
[43] G. 't Hooft, Nucl. Phys. **B75**, 461 (1974).
[44] E. Witten, Nucl. Phys. **B160**, 57 (1979).
[45] G. 't Hooft, Phys. Rev. Lett. **37**, 8 (1976).
[46] I. D. Soares, Phys. Rev. D **17**, 1924 (1978).
[47] E. V. Shuryak and A. Vainshtein, Nucl. Phys. **B199**, 451 (1982).
[48] E. V. Shuryak and A. Vainshtein, Nucl. Phys. **B201**, 141 (1982).
[49] V. Novikov, M. A. Shifman, A. Vainshtein, and V. I. Zakharov, Fortschr. Phys. **32**, 585 (1984).
[50] P. Faccioli and E. V. Shuryak, Phys. Rev. D **64**, 114020 (2001).
[51] R. Bertlmann, G. Launer, and E. de Rafael, Nucl. Phys. **B250**, 61 (1985).
[52] G. Prosperi, M. Raciti, and C. Simolo, Prog. Part. Nucl. Phys. **58**, 387 (2007).
[53] S. Narison and E. de Rafael, Phys. Lett. **103B**, 57 (1981).
[54] V. A. Novikov, M. A. Shifman, A. I. Vainshtein, and V. I. Zakharov, Nucl. Phys. **B165**, 55 (1980).
[55] V. Mathieu, N. Kochelev, and V. Vento, Int. J. Mod. Phys. E **18**, 1 (2009).
[56] D. Dudal, M. S. Guimaraes, and S. P. Sorella, Phys. Rev. Lett. **106**, 062003 (2011).
[57] D. Scharre *et al.*, Phys. Lett. **97B**, 329 (1980).
[58] M. Acciarri *et al.* (L3 Collaboration), Phys. Lett. B **501**, 1 (2001).
[59] G. Gabadadze, Phys. Rev. D **58**, 055003 (1998).
[60] H. Forkel, Braz. J. Phys. **34**, 875 (2004).
[61] L. Faddeev, A. J. Niemi, and U. Wiedner, Phys. Rev. D **70**, 114033 (2004).
[62] S. He, M. Huang, and Q.-S. Yan, Phys. Rev. D **81**, 014003 (2010).
[63] C. Thomas, J. High Energy Phys. 10 (2007) 026.
[64] F. Ambrosino *et al.* (KLOE Collaboration), Phys. Lett. B **648**, 267 (2007).
[65] R. Escribano and J. Nadal, J. High Energy Phys. 05 (2007) 006.
[66] M. S. Chanowitz and S. R. Sharpe, Nucl. Phys. **B222**, 211 (1983); **B228**, 588(E) (1983).
[67] D. Robson, Z. Phys. C **3**, 199 (1980).
[68] B. A. Li, Phys. Rev. D **86**, 017501 (2012).